Synthesis of full-length homodimer αD-VxXXB that targets human α7 nicotinic acetylcholine receptors

Thao N.T. Ho, Nikita Abraham and Richard J. Lewis*

T.N.T. Ho, N. Abraham, Prof. R. Lewis
Centre for Pain Research, Institute for Molecular Bioscience
The University of Queensland
St Lucia, Queensland 4067, Australia
E-mail: r.lewis@uq.edu.au

Experimental Method

Cell culture

Cell culture was performed as previously described [1]. Briefly, SH-SY5Y neuroblastoma cells (a gift from Victor Diaz, Max Plank Institute for Experimental Medicine, Goettingen, Germany) were cultured at 37°C/5% (v/v) CO_2 in RPMI media containing 2 mM L-glutamine and 15% (v/v) FBS. Cells were passaged every 3–5 days using 0.25% trypsin/EDTA at a dilution of 1:5. Experiments were conducted over several months and spanned on average a minimum of 10–20 passages. Responses were not affected by cell passage number with consistent control responses recorded over the duration of experiments as responses.

FLIPR assay

FLIPR assay was performed as previously described [1]. Briefly, cultured SH-SY5Y cells were plated at a density of 100,000 cells per well on black-walled 384-well imaging plates and cultured for 48 h to form a confluent monolayer. Growth media was removed and incubated for 30 min at 37°C with component A of the Calcium 4 assay kit. Intracellular increases in calcium in response to choline selectively activating α7 nAChRs[2] endogenously expressed by the SH-SY5Y cells were recorded . After incubation, the cells were transferred to the FLIPR (Molecular Devices). The changes in fluorescence correlated to intracellular calcium levels were measured using a cooled CCD camera with excitation 470–495 nm, emission 515–575 nm every 1s. Camera gain and intensity were adjusted for each plate of cells yielding a minimum of 1500–2000 arbitrary fluorescence units (AFU) as a baseline fluorescence value. Peptides were added 10 min before applying choline for α7 nAChRs (30 μM). N-(5-Chloro-2,4-dimethoxyphenyl)-N'-(5-methyl-3-isoxazolyl)-urea (PNU120596) to measure activity at the α7 subtype on the FLIPR platform. The channel kinetics are too fast to measure otherwise. All compounds were diluted with physiological salt solution (PSS (mM); 5.9 KCl, 1.5 $MgCl_2$, 1.2 NaH_2PO_4, 5.0 $NaHCO_3$, 140 NaCl, 11.5 glucose, 5 $CaCl_2$, 10 HEPES at pH 7.4). FLIPR data were normalised to the maximum choline (30 μM) response in the SH-SY5Y cells to yield the % Fmax. A four-parameter Hill equation was fitted to the data using GraphPad Prism 9.0. Experiments were performed in triplicate in three independent experiments. The IC_{50} values of three independent experiments are reported as mean with SEM

Binding assays

The ability of VxXXB variants to displace the binding of [^{3}H]-epibatidine to the recombinantly expressed *Ls*-AChBP was examined using the competitive radioligand binding assay [3]. Briefly, [^{3}H]–epibatidine (1 nM final concentration) and increasing concentrations of test ligand in a final volume of 100 μL were incubated in 96-well plates (Flexible PET Microplate, Perkin Elmer) precoated with 1 ng/μL of *Ls*-AChBP per well in binding buffer (phosphate buffered saline (PBS) with 0.05% bovine serum albumin (BSA)). The mixture was then removed and 100 μl of scintillant (Optiphase Supermix, Perkin Elmer) added to each well. Radioactivity was measured with a Wallac 1450 MicroBeta liquid scintillation counter (Perkin Elmer). Competitive radioligand binding data were analysed by a nonlinear, least squares one-site competition fitting procedure using GraphPad Prism 9.0 (GraphPad Software Inc.). The IC_{50} values of three independent experiments are reported as mean with SEM. binding experiments were performed by measuring the bound specific [^{3}H]-epibatidine in the absence or presence of toxin at a concentration twice the toxin IC_{50}. [^{3}H]-epibatidine was added over the concentration range 85 fM–15 nM, with nonlinear regressions fitted in Prism. Saturation radioligand binding data were analysed by the global fitting saturation binding total and non-specific binding curves fitting procedure using GraphPad Prism 9.0 (GraphPad Software Inc.). Experiments were performed in triplicate in three independent experiments.

Data analysis

Comparison of the IC_{50} values between different analogues were carried out by pairwise comparison using an extra sum-of-squares F test with $p < 0.05$ in GraphPad Prism 9.0. Statistical analysis for non-surmountable binding of the concentration-response curves of VxXXB variants binding affinity for *Ls*-AChBP was determined as significant if 95% confidence interval of curve bottom values did not overlap 0%.

Homology modelling

Homology modelling was performed using the project mode of the SWISSMODEL online server [4]. Models of native and synthetic VxXXB were generated by aligning their sequence with the crystal structure of αD-GeXXA. After manually adjusting alignment to improve its quality, the resulting models were energy minimized using the GROSMACS force filed in DEEPVIEW and final models analyzed in PyMol [4] Models of native VxXXB and synthetic VxXXB were also constructed using hetero-oligomer options of ColabFold[5], a user-friendly interface of AlphaFold2 available through notebooks. The structure prediction run by the ColabFold notebook (https://github.com/sokrypton/ColabFold) is powered by AlphaFold2 in combination with a fast, multiple sequence multiple sequence alignments produced by MMseqs2 [6]. Briefly, homologous sequences were searched against existing PDB structures as scaffolds to replace with the new sequences The predicted PDB results were selected based on the predicted confidence (pLDDT) and the expected disulfide frameworks.

Supplementary tables and figures

Table S1. Sequences and masses of synthesised peptides.

Ligation method	Peptide name	Sequence	Theoretical mass (Da)	Observed mass (Da)
	CTD(21–50)	TR(Nle)CGS(Nle)SCPRNGCTCVYHWRRGHGCSCPG#	3261.55	3261.43
	CTD(19–50)	CRTR(Nle)CGS(Nle)CCPRNGCTCVYHWRRGHGCSCPG#	3535.17	3535.13
	NTD(6–18)	CIINTRDSPWGRC* | | *CRGWPSDRTNIIC	3037.52	3037.65
	NTD(1–18)	DDESECIINTRDSPWGRC* | | *CRGWPSDRTNIICESEDD	4186.67	4187.23
Enzyme ligation	NTD(6–18)-[1]	CIINTRDSPWGRC–LPATGG* | | *CRGWPSDRTNIIC	3533.07	3533.45
	CTD(19–50)-[1]	GG–CRTR(Nle)CGS(Nle)CCPRNGCTCVYHWRRGHGCSCPG#	3649.27	3648.34
Hydrazone ligation	NTD(6–18)-[2]	CIINTRDSPWGRC-[$NHNH_2$]* | | *CRGWPSDRTNIIC	3049.76	3049.35
	CTD(19–50)-[2]* Aldehyde	[Aldehyde]–CRTR(Nle)CGS(Nle)CCPRNGCTCVYHWRRGHGCSCPG	3588.34	3589.23
CuAAc ligation	NTD(6–18)-[3]	CIINTRDSPWGRC– [Prg]* | | *CRGWPSDRTNIIC	3131.32	3131.34
	CTD(19–50)-[3]	[Aza]–CRTR(Nle)CGS(Nle)CCPRNGCTCVYHWRRGHGCSCPG#	3653.34	3653.45
KAHA ligation	NTD(6–18)-[4]	CIINTRDSPWGRC–[LeuKA]* | | *CRGWPSDRTNIIC	3176.78	3176.34
	NTD(1–18)-[4]	DDESECIINTRDSPWGRC–[LeuKA]* | | *CRGWPSDRTNIICESEDD	4326.34	4329.64
	NTD(1–18)-[5]	DDESEECIINTRDSPWGRC–[LeuKA]* | | *[LeuKA]–CRGWPSDRTNIICESEDD	4468.44	4470.23
	CTD(19–50)-[4]	[Hse]–CRTR(Nle)CGS(Nle)CCPRNGCTCVYHWRRGHGCSCPG#	3646.67	3646.34
Ligated variants	VxXXB N(6-18)C		6750.80	6756.90
	VxXXB N(1-18)C		7901.77	7912.87
	VxXXB CN(1-18)C		11636.12	11651.23

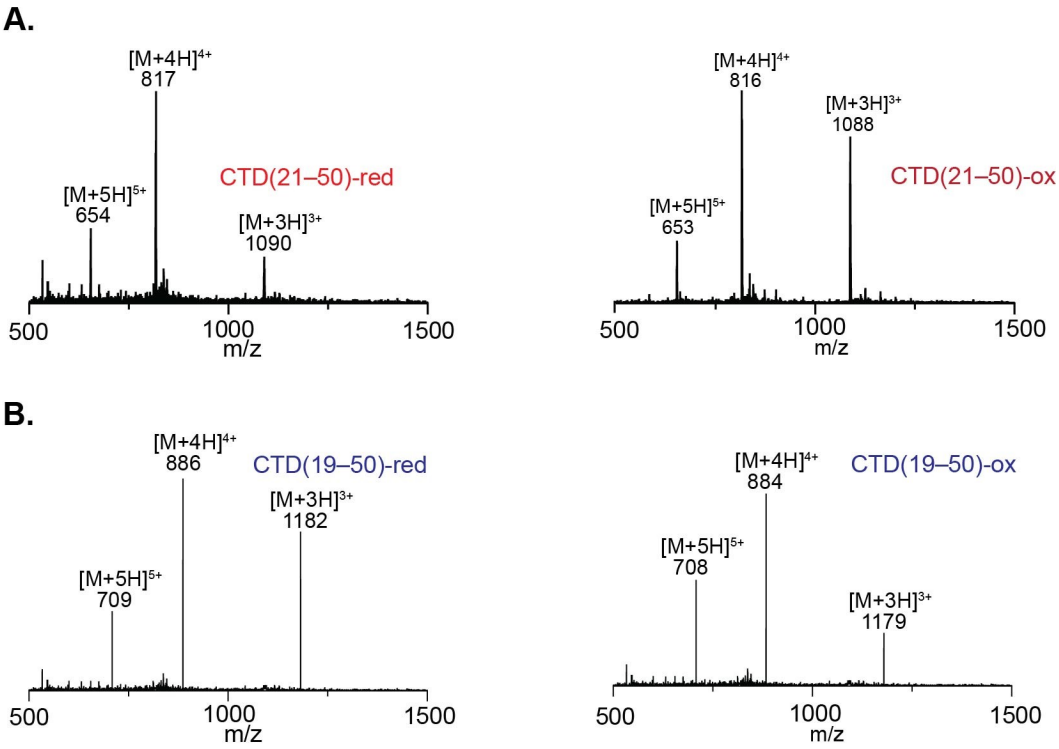

Figure S1. ESI-MS spectra of VxXXB CTD (A) and NTD variants (B) observed with ESI-MS (positive ion-mode) on a high-resolution ABSciex API5000 LC/MS/MS.

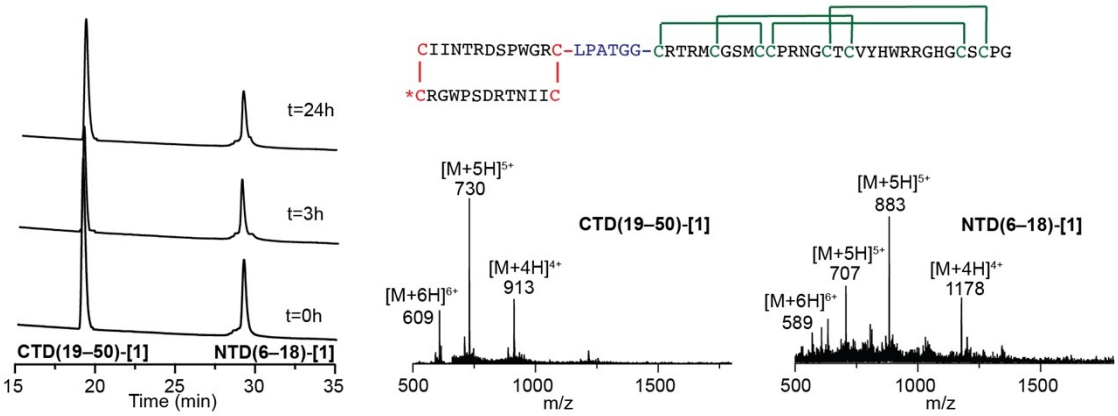

Figure S2. Characterisation of the ligation of VxXIIB N(6–18)C with sortase enzyme ligation. Sortase enzyme ligation progress monitored by RP-HPLC chromatogram of VxXIIB CTD(19–50)–[1] and NTD(6–18)–[1] at different time points (right). Monoisotopic mass of VxXIIB CTD(19–50)-[1] and VxXIIB NTD(1–18)-[1] detected by ESI-MS on an ABSciex API5000 LC/MS/MS.

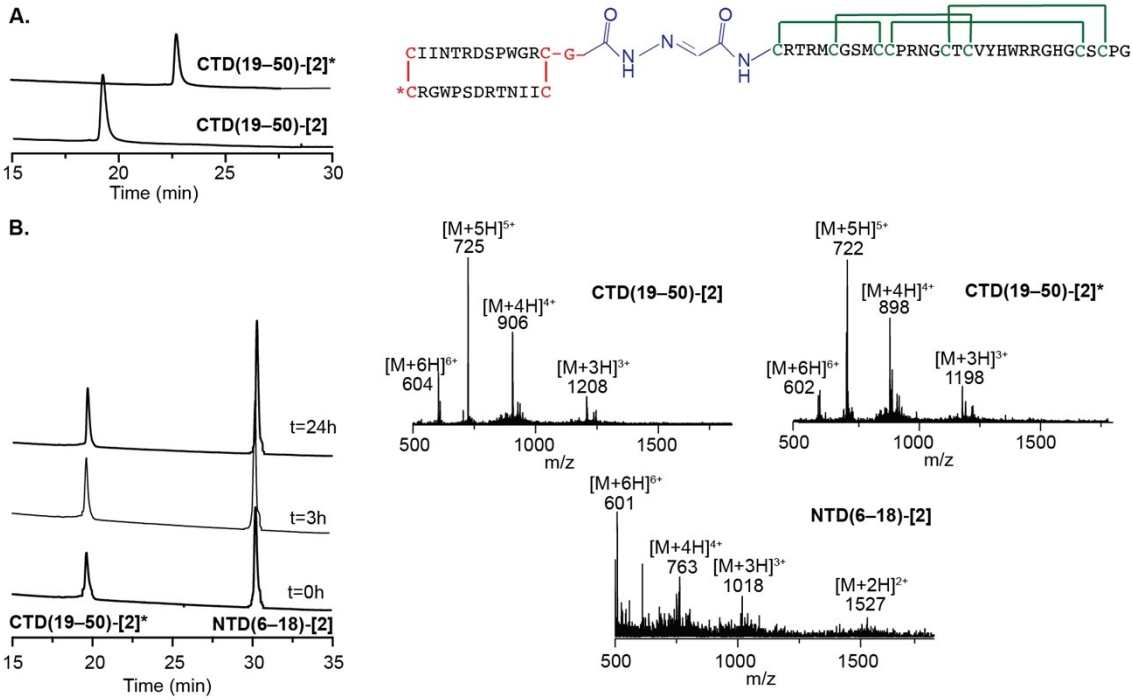

Figure S3. Characterisation of the ligation of VxXIIB N(6–18)C with hydrazone ligation. (A) N-terminal Serine of VxXIIB CTD(19–50)–2 (lower) was converted to aldehyde moiety CTD(19–50)–[2]* (upper) (a) and the sequence of ligated VxXIIB N(6–18)C achieved with hydrazone ligation. (B) Hydrazone ligation progress monitored by RP-HPLC chromatogram of VxXIIB CTD(19–50)–[2]* and VxXIIB NTD(6–18)–[2] at different time points (right). Monoisotopic mass of VxXIIB CTD(19–50)-[2], VxXIIB CTD(19–50)-[2]* and VxXIIB NTD(6–18)-[2] detected by ESI-MS on an ABSciex API5000 LC/MS/MS.

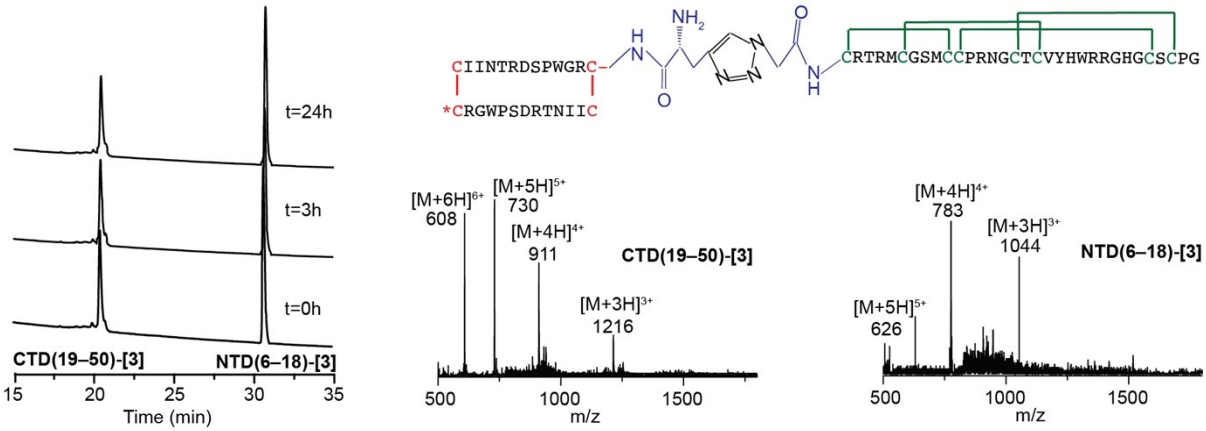

Figure S4. Characterisation of the ligation of VxXIIB N(6–18)C with CuAAc ligation. CuAAC ligation progress monitored by RP-HPLC chromatogram of VxXIIB CTD(19–50)-[3] and NTD(6–18)-[3] at different time points (right). Monoisotopic mass of VxXIIB CTD(19–50)-[3] and VxXIIB NTD(6–18)-[3] detected by ESI-MS on an ABSciex API5000 LC/MS/MS.

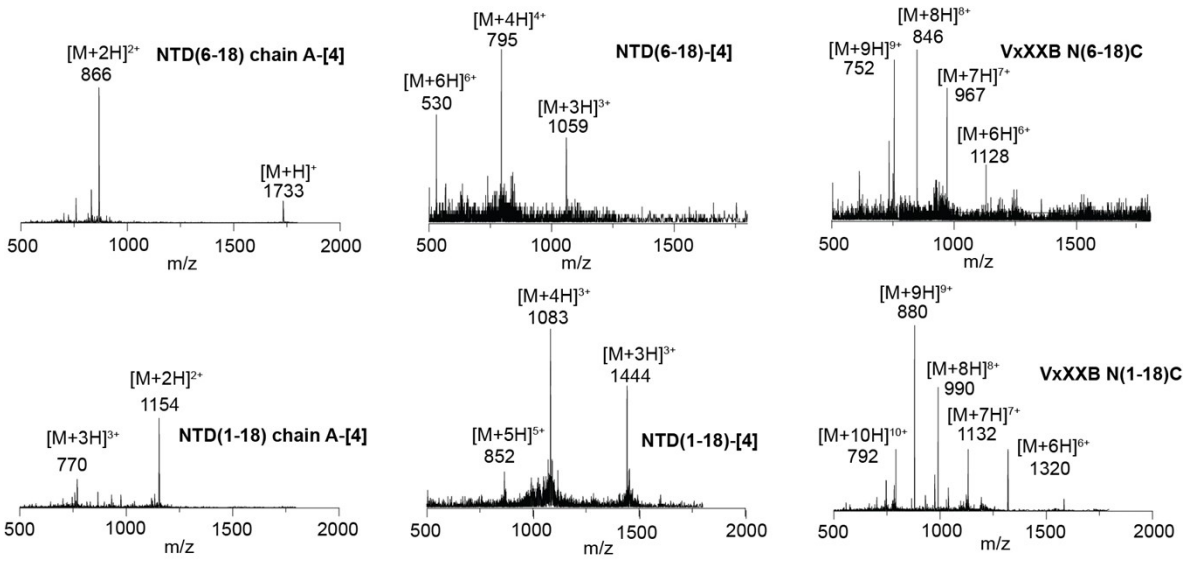

Figure S5. ESI-MS spectra of VxXIIB variants with KAHA ligation: each chain of NTD(6–18)-[4], NTD(1–18)-[4], the fully oxidised NTD(6–18)-[4], NTD(1–18)-[4] and the ligated VxXIIB N(6–18)C and VxXIIB N(1–18)C observed with ESI-MS (positive ionmode) on a high-resolution ABSciex API5000 LC/MS/MS.

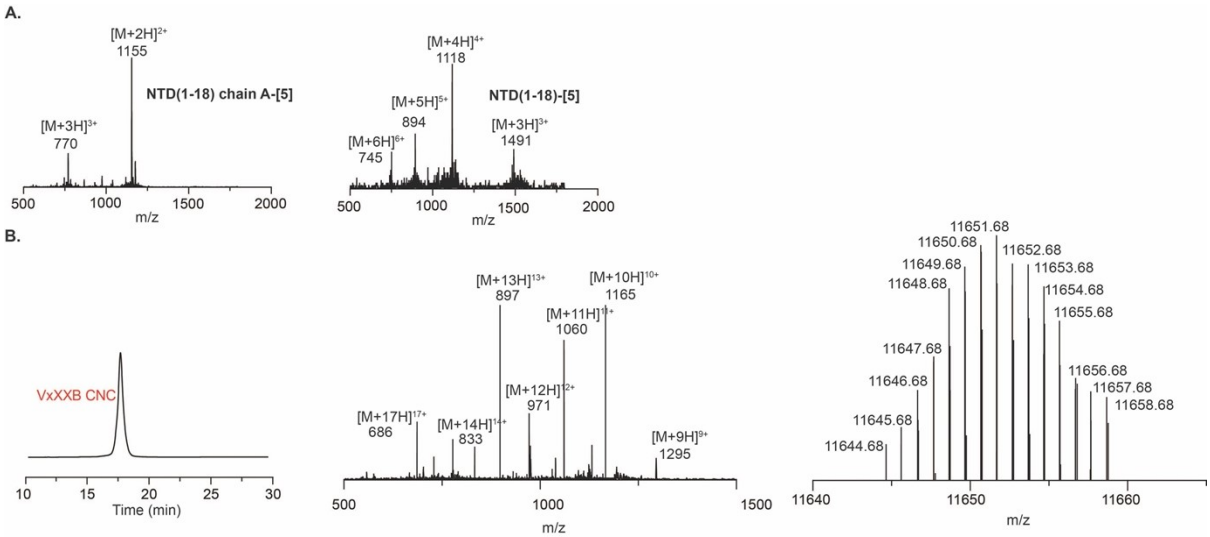

Figure S6. Characterisation of VxXIIB CN(1–18)C. (A) ESI-MS spectra of each chain of NTD(1–18)-[5] and the fully oxidised NTD(1–18)-[5] observed with ESI-MS (positive ionmode) on a high-resolution ABSciex API5000 LC/MS/MSAnalytical. (B) RP-HPLC chromatogram and ESI-MS spectrum observed with LC-ESI-MS (positive ion mode) and reconstructed mass spectrum for VxXIIB CN(1–18)C using a high-resolution TripleTOF 5600 mass spectrometer (AB Sciex).

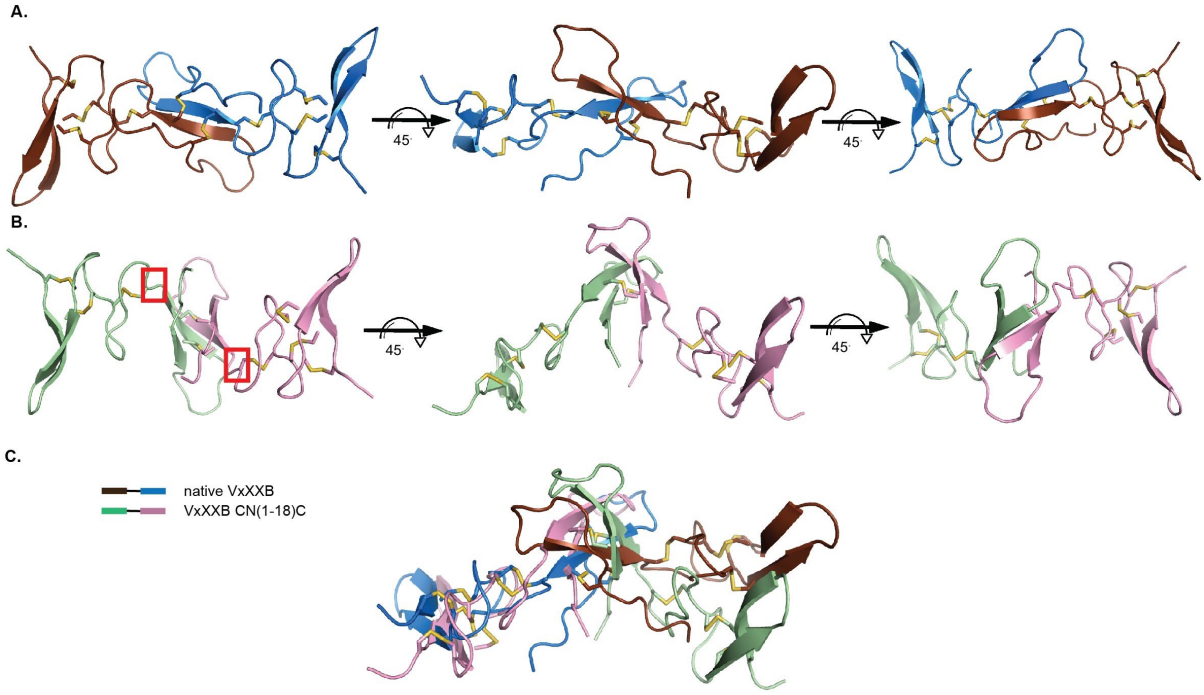

Figure S7. Model of native VxXXB (A) and synthetic VxXXB CNC (B) generated from AlphaFold. (C) The alignment between native VxXXB and VxXXB CNC viewed from front (upper) and top (lower). The KAHA-inserted -L^{h}S- is highlighted in red boxes.

References

1. M. C. Inserra, S. N. Kompella, I. Vetter, A. Brust, N. L. Daly, H. Cuny, D. J. Craik, P. F. Alewood, D. J. Adams and R. J. Lewis, *Biochem. Pharmacol.*, 2013, **86**, 791-799.
2. M. Alkondon, E. F. Pereira, W. S. Cortes, A. Maelicke and E. X. Albuquerque, *Eur. J. Neurosci.*, 1997, **9**, 2734-2742.
3. N. Abraham, B. Paul, L. Ragnarsson and R. J. Lewis, *PLoS One*, 2016, **11**, e0157363.
4. N. Guex, M. C. Peitsch and T. Schwede, *Electrophoresis*, 2009, **30 Suppl 1**, S162-173.
5. M. Mirdita, S. Ovchinnikov and M. Steinegger, *bioRxiv*, 2021, DOI: 10.1101/2021.08.15.456425, 2021.2008.2015.456425.
6. M. Mirdita, M. Steinegger and J. Söding, *Bioinformatics*, 2019, **35**, 2856-2858.